

# A Molecular View of Cholesterol-Induced Condensation in a Lipid Monolayer

Mischa Bonn,<sup>\*,†,‡</sup> Sylvie Roke,<sup>‡</sup> Otto Berg,<sup>‡</sup> Ludo B.F. Juurlink,<sup>‡</sup> Amalia Stamouli,<sup>‡</sup> and Michiel Müller<sup>§</sup>

FOM Institute for Atomic and Molecular Physics, Kruislaan 407, 1098 SJ, Amsterdam, The Netherlands, Leiden Institute of Chemistry, Leiden University, P.O. Box 9502, 2300 RA Leiden, The Netherlands, and Swammerdam Institute for Life Sciences, University of Amsterdam, P.O. Box 94062, 1090 GB Amsterdam, The Netherlands

Received: October 19, 2004; In Final Form: November 12, 2004

We investigate the intermolecular interactions in a mixed phospholipid/cholesterol monolayer using the surface-specific technique of vibrational sum frequency generation. This technique allows us to monitor the conformational and orientational order in the phospholipid as the surface pressure and cholesterol content are varied. We find a disproportionally large increase in phospholipid molecular order upon addition of relatively small amounts of cholesterol, a witness to the condensation effect at the molecular level.

The cholesterol content of the plasma membrane of eukaryotic cells can be as high as 40 mol %.<sup>1</sup> Cholesterol is a key membrane constituent that provides the cell with a means to modify essential membrane properties.<sup>2,3</sup> A detailed understanding of the effect of cholesterol on the structure and organization of lipid layers is therefore essential for a thorough comprehension of membranes, and accordingly has received much attention.<sup>2–4</sup> Previous studies have demonstrated that, indeed, cholesterol plays a key role in controlling membrane fluidity, permeability, and mechanical strength. In particular, the incorporation of cholesterol in membrane layers leads to an increased ordering of the hydrocarbon chains of lipids and to a reduction in the area per molecule (partial molar area) for monolayers, the so-called condensation effect. In addition, cholesterol broadens and eventually eliminates the liquid-to-solid-phase transition of phospholipid membranes.<sup>2–4</sup>

Various techniques have been used to explore the molecular nature of cholesterol/phospholipid interactions that give rise to the modified behavior. NMR studies have provided detailed information on the important role of hydrophobic interactions between cholesterol and phospholipids (see, e.g., refs 2 and 5) and on the ordering of lipid acyl chains and possible lipid phase separation mechanisms.<sup>6–8</sup> The existence of cholesterol/phospholipid condensed complexes has been inferred from fluorescence phase separation studies in lipid monolayers,<sup>9,10</sup> and detailed information on possible hydrogen-bond formation between cholesterol and various lipids has been obtained using molecular dynamics simulations.<sup>11,12</sup>

Vibrational sum frequency generation (VSFG) has proven to be ideally suited to study order and orientation on a molecular level in lipid layer systems.<sup>13–18</sup> Here, we employ VSFG to systematically study the effect of cholesterol on a model lipid system: a monolayer of L-1,2-dipalmitoyl-sn-glycero-3-phosphocholine (DPPC, structure depicted in ref 13). We find cholesterol-induced ordering of the phospholipid tail, a distinct molecular signature of the well-known condensation effect,

already occurring at remarkably low cholesterol content. Previous second harmonic studies have demonstrated that the presence of 50% cholesterol in a phospholipid bilayer increases the molecular transit time across the bilayer by a factor of 6, compared to a cholesterol-free bilayer.<sup>19</sup>

The VSFG experiments were performed using p-polarized, 120 fs (3  $\mu$ J) infrared pulses with a spectral width of 180  $\text{cm}^{-1}$  (fwhm), centered at 2930  $\text{cm}^{-1}$ , and s-polarized, 3.5  $\mu$ J, 800 nm (VIS) pulses with a spectral width of 11  $\text{cm}^{-1}$  (repetition rate: 1 kHz). The IR and VIS pulses were focused down to 0.4 and 0.8 mm beamwaists, respectively, and were both incident at a 65° angle with respect to the surface normal. Spectra were obtained by focusing the generated SFG light onto the entrance slit of a spectrometer, which dispersed it onto an intensified charge coupled device (CCD) camera. Spectra are averages of 100 s.

For the monolayers, binary solutions of DPPC (obtained from Avanti Polar Lipids, Birmingham, AL) and deuterated cholesterol (25,26,26,26,27,27,27 -D7, obtained from Cambridge Isotope Laboratory, Andover, MA) were spread from a low concentration chloroform solution (Fisher HPLC grade) onto distilled Millipore filtered water (18 M $\Omega$  cm resistivity) of pH 7, in a home-built Teflon trough (dimensions 5  $\times$  40  $\text{cm}^2$ ). The surface pressure of the system was monitored with a commercial surface tensiometer (Kibron, Finland). Care was taken to minimize exposure of samples to air during preparation of the monolayer. VSFG measurements of the monolayer were taken in compression mode, to ensure thermodynamic equilibrium. Fluorescence microscopy revealed homogeneous lipid distributions at the length scale of the VSFG experiments ( $\sim$ 400  $\mu\text{m}$ ) at all stages of compression for cholesterol concentrations exceeding 10 mol %. The small heterogeneities ( $<10 \mu\text{m}$ ) reported by others<sup>20,21</sup> for these lipid compositions were below our imaging resolution.

Two typical experimental runs are depicted in Figure 1. The two panels depict VSFG spectra in the C–H stretching region as a function of surface area per DPPC molecule, without (left) and with 20 mol % cholesterol (right). For all data sets shown in this report, the spectrum with the smallest area per DPPC

\* Corresponding author. E-mail: bonn@amolf.nl.

<sup>†</sup> FOM Institute for Atomic and Molecular Physics.

<sup>‡</sup> Leiden University.

<sup>§</sup> University of Amsterdam.

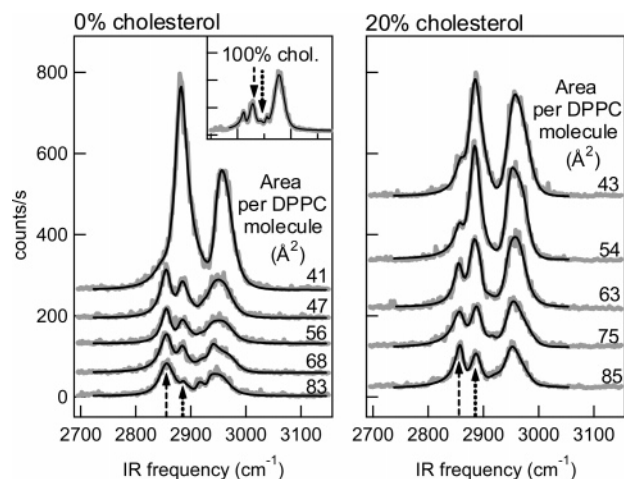


**Figure 1.** SFG spectra (gray lines) and fits (black lines) of DPPC monolayers as a function of surface area per DPPC molecule in the absence (left panel), and presence of 20% cholesterol (right panel). Clearly, with no cholesterol present, the intensity of the symmetric  $\text{CH}_3$  stretch vibration (dotted arrow) increases abruptly when full compression is reached. With 20% cholesterol, the increase is gradual. For the latter, some of the signal originates from cholesterol itself, which is not fully deuterated. Its contribution to the symmetric  $\text{CH}_3$  stretch signal is nil, as shown in the inset for a compressed cholesterol monolayer. Its contribution to the symmetric  $\text{CH}_2$  stretch signal (dashed arrow) is significant for cholesterol contents exceeding 20%, and corrected for in the analysis.

molecule corresponds to a fully compressed layer with a surface pressure of 40 mN/m.

From the data in Figure 1, it is evident that there is a marked effect of cholesterol on the phospholipid behavior. In what follows, we will focus on the SFG signal assigned to the symmetric  $\text{CH}_2$  and  $\text{CH}_3$  stretch vibrations of the phospholipids, the frequencies of which are indicated as dashed ( $\text{CH}_2$ :  $\sim 2850\text{ cm}^{-1}$ ) and dotted ( $\text{CH}_3$ :  $\sim 2880\text{ cm}^{-1}$ ) arrows, respectively, in Figure 1. The SFG signal from a monolayer of pure (partially deuterated) cholesterol (shown for a compressed layer in the inset in Figure 1) reveals no effects of intermolecular interactions: the shape of the spectrum remains unchanged with varying density, and the spectral intensity simply scales with the square of cholesterol density. Cholesterol has a negligibly small resonance at the symmetric  $\text{CH}_3$  stretch vibrational frequency, simplifying our study. The symmetric  $\text{CH}_2$  intensity of cholesterol is sufficiently small to be negligible compared to the signal from the phospholipids up to  $\sim 20\text{ mol } \%$  cholesterol. For higher fractions, we correct for the signal from cholesterol, neglecting possible interference effects between the  $\text{CH}_2$  signals of cholesterol and DPPC by assuming in our analysis that these are independent and additive.

Both with and without cholesterol, the signal is dominated by the lipid acyl chain  $\text{CH}_3$  stretch vibrations when the layer is fully compressed. Owing to the selection rules of SFG the  $\text{CH}_2$  resonances are not SFG-active for a fully stretched, all-trans alkyl chain.<sup>22</sup> Inversely, the appearance of  $\text{CH}_2$  stretch intensity must be due to gauche defects. This means that the symmetric  $\text{CH}_2$  stretch intensity is a direct measure for the *conformational disorder* in the lipid chain. The two  $\text{CH}_2$  groups on the DPPC headgroup are not detectable, as evidenced from selective isotopic substitution of the acyl chain. The  $\text{CH}_3$  intensity is greatly enhanced when the vibrational dipoles are aligned, as VSFG is a coherent process. Thus, the  $\text{CH}_3$  intensity is a very sensitive probe of the *orientational order* in the lipid tail. Note that the methylene  $\text{CH}_2$  stretch is sensitive to the appearance of gauche defects in the chain, whereas the orientational order

probed by the methyl stretch is influenced by both the gauche kinks as well as possibly the orientational motion of the lipid molecule as a whole. As will be shown below, the correlation between the two provides insight into the relative importance of gauche kinks on the orientational order.

It is evident from Figure 1 that the effect of cholesterol on phospholipid orientational order is dramatic: whereas for pure DPPC the  $\text{CH}_3$  intensity dominates only at very high compression, and disappears very suddenly for larger surface areas, the variations in  $\text{CH}_3$  intensity are much more gradual for the sample with 20% cholesterol.

This effect can readily be quantified through the intensities of the different modes obtained from established fitting procedures (black lines in Figure 1),<sup>13,23</sup> the results of which are summarized in Figure 2. Panel A demonstrates that the decrease in  $\text{CH}_3$  intensity with expansion of the monolayer is gradual in the presence of cholesterol, as discussed in the previous paragraph. Panel B reveals that the  $\text{CH}_2$  intensity increases very steeply upon decompression to level off at higher surface area; the surface area where this transition occurs depends strongly on cholesterol content. The results are re-plotted in panel C of Figure 2 to reveal that there is a negative correlation between the  $\text{CH}_3$  and  $\text{CH}_2$  intensities, irrespective of the cholesterol concentration. This indicates that the main factor in the decrease in the orientational order is the appearance of gauche defects, and not tilting of entire lipid molecules. This observation is in agreement with previous reports that in phosphatidylcholine bilayers the phospholipid headgroup is oriented approximately parallel to the plane of the bilayer<sup>2,3</sup> and that the insertion of cholesterol into the membrane does not change this conformation.<sup>2,3</sup> Note that the  $180\text{ cm}^{-1}$  broad IR pulse is centered around  $2930\text{ cm}^{-1}$  so that the  $2880\text{ cm}^{-1}$  mode is detected slightly more efficiently than the  $2850\text{ cm}^{-1}$  mode. This does not affect our results and conclusions, however.

Two important observations can be made from our data. The first is that, despite the finite area taken up by a cholesterol molecule, a DPPC monolayer containing 10% cholesterol is more compressible than a monolayer of pure DPPC. This well-known effect illustrates the influence of cholesterol on the packing state of DPPC molecular chains and is generally referred to as the “condensation effect”. The second, more surprising observation is that an increase of the molecular surface area  $A$  from 41 to  $47\text{ Å}^2/\text{molecule}$  has dramatic effects on the spectra of pure DPPC, whereas, when 10 mol % cholesterol is present, the change in  $A$  from 40 through 44 to  $50\text{ Å}^2/\text{molecule}$  hardly affects the spectra: the onset of disorder in the lipid tail does not become apparent until  $A = 60\text{ Å}^2/\text{molecule}$ . Note that the pressure isotherms for pure DPPC and (DPPC+10% chol) are practically indistinguishable in this region.<sup>20</sup> Clearly, the presence of 10% cholesterol affects the changes in the phospholipid orientational and conformational disorder quite dramatically: for a dilute DPPC layer, the increase in order is much larger when cholesterol is added than when an equimolar amount of DPPC is added, despite the larger apolar volume of DPPC compared to cholesterol. This is most clearly observed for the sample with 10% cholesterol and constitutes a direct molecular observation of the long-range influence of the packing state of DPPC molecular chains. It also demonstrates that one cholesterol molecule affects many DPPC molecules. Indeed, the changes upon adding additional cholesterol to the system (20–50%) are relatively small compared to the step from 0 to 10%.

Hydrophobic interactions appear to dominate these cholesterol–phospholipid interactions. Although hydrogen-bonding between the hydroxyl group of cholesterol and carbonyl groups of the

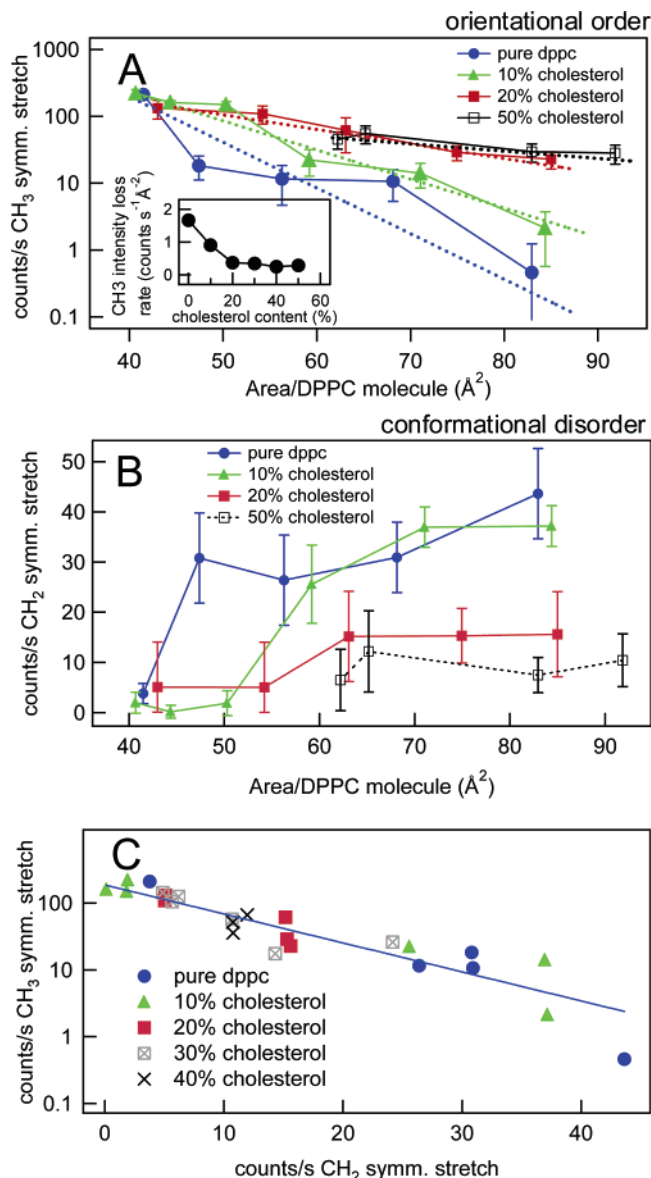


**Figure 2.** Summary of the data, as obtained from the fits shown in Figure 1. Panels A and B depict the peak intensity in counts/second of the symmetric CH<sub>3</sub> and CH<sub>2</sub> stretch, respectively, on a logarithmic and linear scale. The CH<sub>3</sub> intensity, a good measure for the orientational order of the terminal methyl groups, decays much more slowly in the presence of cholesterol (Panel A). The inset in panel A depicts the slopes of the dotted best-fit lines as a function of cholesterol concentrations. The CH<sub>2</sub> intensity, a good measure for the conformational disorder in the alkyl chain, increases at a larger surface area when cholesterol is present (panel B). Error bars denote  $\pm\sigma$  obtained from the fitting procedure. The clear anti-correlation between the CH<sub>3</sub> and CH<sub>2</sub> stretch intensities shown in panel C indicates that the increase in conformational disorder (panel B) is indeed the main cause of the decrease in orientational order (panel A).

lipid acyl chains, or possibly the phosphate group in the sn-3 position cannot be ruled out, hydrogen-bond formation between cholesterol and water is considered more likely.<sup>2,24</sup> The largest contribution to the cholesterol–phospholipid interaction is therefore expected to originate from van der Waals forces

between the cholesterol and the lipid chains within the bilayer hydrophobic core. The importance of the hydrophobic core of cholesterol is also emphasized in models of superlattice formation of cholesterol in phosphocholine bilayers<sup>25</sup> where cholesterol is thought to fill the hydrophobic pockets underneath the relatively large DPPC headgroup. This tendency could also explain the observed condensing effect.

Summarizing, we have presented the first surface-specific vibrational study of phospholipid–cholesterol interactions, which reveals the molecular signature of the well-known condensation effect and demonstrates the ordering influence by cholesterol, in both the lipid conformation and orientation. Future investigations will be aimed at elucidating the relative contribution to cholesterol–phospholipid interactions from, on one hand, van der Waals forces and hydrophobic forces and, on the other hand, hydrogen bonding of the cholesterol hydroxyl group to the polar headgroup, e.g. by investigating the different vibrational modes in both the lipid molecules and cholesterol.

**Acknowledgment.** We are grateful to S. Woutersen for his helpful comments. This work is part of the research program of the “Stichting voor Fundamenteel Onderzoek der Materie (FOM)”, which is financially supported by the “Nederlandse organisatie voor Wetenschappelijk Onderzoek (NWO)”.

## References and Notes

- (1) Munro, S. *Cell* **2003**, *115*, 377.
- (2) Demel, R. A.; Kruffy, B. D. *Biochim. Biophys. Acta* **1976**, *457*, 109.
- (3) Ohvo-Rekilä, H.; Ramstedt, B.; Leppimäki, P.; Slotte, J. P. *Prog. Lipid Res.* **2002**, *41*, 66.
- (4) McMullen, T. P. W.; Lewis, R. N. A. H.; McElhaney, R. N. *Curr. Opin. Colloid Interface Sci.* **2004**, *8*, 459.
- (5) Bhattacharya, S.; Haldar, S. *Biochim. Biophys. Acta* **2000**, *1467*, 39.
- (6) Vist, M. R.; Davis, J. H. *Biochemistry* **1990**, *29*, 451.
- (7) Heerklotz, H. *Biophys. J.* **2002**, *83*, 2693.
- (8) Veatch, S. L.; Polozov, I. V.; Gawrisch, K.; Keller, S. L. *Biophys. J.* **2004**, *86*, 2910.
- (9) Radhakrishnan, A.; McConnell, H. M. *Biophys. J.* **1999**, *77*, 1507.
- (10) Radhakrishnan, A.; Anderson, T. G.; McConnell, H. M. *Proc. Nat'l. Acad. Sci. U.S.A.* **2000**, *97*, 12422.
- (11) Róg, T.; Pasenkiewicz-Gierula, M. *Biophys. J.* **2001**, *81*, 2190.
- (12) Pandit, S. A.; Bostick, D.; Berkowitz, M. L. *Biophys. J.* **2004**, *86*, 1345.
- (13) Roke, S.; Schins, J.; Müller, M.; Bonn, M. *Phys. Rev. Lett.* **2003**, *90*, 128101.
- (14) Liu, J.; Conboy, J. C. *J. Am. Chem. Soc.* **2004**, *126*, 8376.
- (15) Liu, J.; Conboy, J. C. *J. Am. Chem. Soc.* **2004**, *126*, 8894.
- (16) Petralli-Mallow, T.; Briggman, K. A.; Richter, L. J.; Stephenson, J. C.; Plant, A. L. *Proc. SPIE* **1999**, *3858*, 25.
- (17) Walker, R. A.; Conboy, J. C.; Richmond, G. L. *Langmuir* **1997**, *13*, 3070.
- (18) Doyle, A. W.; Fick, J.; Himmelhaus, M.; Eck, W.; Graziani, I.; Prudovsky, I.; Grunze, M.; Maciag, T.; Neivandt, D. J. *Langmuir* **2004**, *20*, 8961–8965.
- (19) Yan, E. C. Y.; Eiseenthal, K. B. *Biophys. J.* **2000**, *79*, 898.
- (20) Yuan, C.; Johnston, L. J. *J. Microscopy* **2002**, *205*, 136.
- (21) Weis, R. M.; McConnell, H. M. *J. Phys. Chem.* **1985**, *89*, 4453.
- (22) Guyot-Sionnest, P.; Hunt, J. H.; Shen, Y. R. *Phys. Rev. Lett.* **1989**, *59*, 1597.
- (23) Hunt, J. H.; Guyot-Sionnest, P.; Shen, Y. R. *Chem. Phys. Lett.* **1987**, *133*, 187.
- (24) McMullen, T. P. W.; McElhaney, R. N. *Curr. Opin. Colloid Interface Sci.* **1996**, *1*, 83.
- (25) Huang, J.; Feigenson, G. W. *Biophys. J.* **1999**, *76*, 2142.